https://doi.org/10.5194/egusphere-2026-1725
Preprint. Discussion started: 27 April 2026

Environmental moisture and stability controls on raindrop size distribution within convective clouds under sheared conditions

Takashi Unuma

Meteorological Research Institute, Japan Meteorological Agency, Tsukuba, Ibaraki, Japan

Correspondence: Takashi Unuma (unuma@mri-jma.go.jp)

Abstract. Environmental conditions significantly influence the intensity of organised convective systems. However, variations in factors such as temperature, humidity, and vertical shear suggest that non-linear relationships may exist between these systems and their environments. To address gaps in these variations, it is crucial to understand the cloud microphysical processes inherent to convective systems. In this study, we conducted numerical experiments using the Weather Research and Forecasting model in idealised setups with a spectral-bin microphysical scheme that explicitly handles drop-size distributions. The initial conditions included variations in humidity, temperature lapse rates, and vertical wind shear that reflect observed relationships. The results showed that larger temperature lapse rates produced larger raindrops, resulting in stronger rainfall intensity. Increased moisture in the lower troposphere led to stronger rainfall intensity, driven by a larger concentration of smaller raindrops and increased liquid water content. The magnitude of vertical shear generally causes fluctuations in the drop size distribution within convective clouds. Particularly, weaker vertical shear tends to inhibit the propagation of convective clouds, reduce vertical variations in the drop-size distribution within them, and may reduce the raindrop evaporation rate, thereby increasing rainfall amounts. These findings provide valuable insights that could enhance operational quantitative precipitation estimation and improve the microphysical schemes used in numerical weather models.

1 Introduction

The intensity of organised precipitating systems, including mesoscale convective systems, has been diagnosed using indicators such as updraughts and rainfall intensity. Differences in updraughts have investigated to show distinct variations over between the tropics and mid-latitudes, resulting from differences in buoyancy fields (e.g., Lucas et al., 1994). This point has also examined in numerical experiments simulating squall lines (e.g., James et al., 2006; Houston and Niyogi, 2007; Takemi, 2007). Much previous research has focused on phenomena associated with strong updraught regions, such as supercells and squall lines, primarily occurring over the United States Great Plains (e.g., Morrison et al., 2012; Xue et al., 2017; Kumjian et al., 2014), where processes involving the ice phase can be significant (Morrison et al., 2015). Conversely, for extreme heavy rainfall associated with weaker updraughts, processes involving warm rain below the melting layer have been highlighted as crucial (e.g., Ding et al., 2023; Wang et al., 2023; Gupta et al., 2023). Particularly in Japan, the importance of a moist environmental field for convective clouds producing heavy rainfall has been highlighted (e.g., Unuma and Takemi, 2016a; Kato, 2020).

https://doi.org/10.5194/egusphere-2026-1725
Preprint. Discussion started: 27 April 2026

Convective systems in humid environments have been found to exhibit varying development altitudes for convective clouds, primarily depending on the surrounding atmosphere's humidity (e.g., Johnson et al., 1999; Kikuchi and Takayabu, 2004). In Japan, it has been noted that such moist lower-level conditions can be favourable for the development of slow-moving convective systems (Unuma and Takemi, 2016a, b). Takemi (2015) demonstrated that in moist environments, numerous vertical flow cores with little dilution from the surrounding air can exist. Li et al. (2017) demonstrated that lower-level moisture leads to a monotonically increasing total rainfall, followed by the formation of a cold air mass near the surface that restricts the development of subsequently emerging convective clouds. Schumacher (2015) showed that even slight variations in near-surface water vapour content can significantly influence surface rainfall. Schumacher and Peters (2017) further conducted experiments in which they applied a slight increase in water vapour content to the initial conditions. The results showed that the rainfall amount generated by the convective system increased as the water vapour perturbation grew larger; however, the change in precipitation did not vary proportionally with the magnitude of the water vapour perturbation. The fact that both the amount and location of convective system's precipitation are highly sensitive to slight changes in low-level water vapour indicates that even minor water vapour errors in numerical weather prediction models can lead to significant errors in predicting convective system location and behaviour. From a forecasting perspective, Kato et al. (2003) conducted numerical simulations of heavy rainfall events that were forecast incorrectly during a specific observation period, indicating the importance of water vapour accumulation in the lower troposphere. These effects should be discussed, including cloud microphysical properties.

Rainfall intensity, as an integral value from the perspective of drop size distribution (DSD), is expected to show apparent differences between the tropics and mid-latitudes in both drop size and number concentration (e.g., Bringi et al., 2003; Dolan et al., 2018; Unuma et al., 2025). Regarding DSDs, Kumjian et al. (2014) examined that parameterisations commonly used in cloud microphysical schemes may yield distributions sensitive to rainfall intensity and biased towards tropical conditions compared to mid-latitude conditions. Seifert et al. (2005) demonstrated that including collisional breakup characteristics reduces surface rainfall intensity but enhances the convection that is subsequently generated. Morrison et al. (2012) showed that domain-averaged precipitation increases when collisional breakup process is efficient. Diehl et al. (2025) proposed a re-parameterisation of collisional breakup characteristics based on laboratory experiments and evaluated its impact using cloud models. They showed that including collisional breakup reduces the number of maximum raindrops, delays precipitation onset, decreases total rainfall, and locally alters precipitation distribution. Such nonlinear relationships may be inherent within convective systems; however, few studies have examined these effects whilst accounting for environmental conditions in the surrounding atmosphere.

From the perspective of Quantitative Precipitation Estimation (QPE), when translating observed values at specific altitudes into areal distributions of surface rainfall, it is essential to capture variations in the vertical distribution of DSDs accurately as much as possible. In QPE, adjustments are made by applying appropriate precipitation-observation relationships, correcting for horizontal advection and vertical effects, and applying adjustments based on rain gauge data. Among these, the Japan Meteorological Agency's QPE system, due to its high density of rain gauges, incorporates not only appropriate precipitation-observation relationships but also horizontal and vertical corrections through rain gauge adjustments (Nagata, 2011). On the other hand, since it is necessary to wait for rain gauge data to be received during product generation, timeliness is often com-

https://doi.org/10.5194/egusphere-2026-1725
Preprint. Discussion started: 27 April 2026

promised. Furthermore, actual physical processes can occur at scales smaller than the observational resolution. Fortunately, the deployment of polarimetric radar is progressing in many countries, making high-temporal and spatial resolution observational data increasingly available. Especially in Japan, it has become clear that vertical variations of DSDs are significant as investigated in (Unuma et al., 2023; Unuma, 2024, 2025), suggesting that vertical corrections are important for QPE. In this regard, researches on vertical variations related to cloud microphysical processes has been conducted from various perspectives.

Hu and Srivastava (1995) demonstrated that incorporating raindrop evaporation effects into the rain shaft model narrows the spectral width of the drop-size distribution. Li and Srivastava (2001) found that whilst evaporation has a negligible effect on the large-diameter end of the drop-size distribution, allowing it to approximately maintain an exponential distribution, its impact on the number concentration at the small-diameter end is significant. Consequently, the mean diameter of the drop size distribution may increase. Seifert (2008) found that evaporation fundamentally reduces both the spectral width and the mass-weighted mean diameter on the size distribution. However, when the raindrop size distribution contains a large proportion of drizzle-sized droplets, the removal of droplets and their conversion to raindrops cancel each other out, keeping the spectral width and mass-weighted mean drop size nearly constant. For example, Xie et al. (2016) shows raindrops smaller than 1 mm in diameter tend to evaporate as they fall toward the ground when the relative humidity near the ground is relatively low (< 60 $\%$). The estimated rainfall intensity at an altitude of $2\,\mathrm{km}$ tends to decrease near the ground as the differential reflectivity (Z_{DR}) value decreases. Paukert et al. (2019) demonstrated that the shape of the raindrop size distribution is primarily determined by sedimentation and evaporation. However, in heavy rain, it is significantly influenced by collisional coalescence and collisional fragmentation of raindrops rather than evaporation. These results suggest that, whilst raindrop size distributions are generally susceptible to evaporation, this is not necessarily the case during heavy rain.

At present, the correlations between environmental conditions and the DSD parameters were known to exist as an observational fact (Unuma, 2025); however, the physics linking the environmental conditions of the surrounding atmosphere to cloud microphysical processes in a convective cloud is not yet fully understood. With the use of polarimetric weather radar, whilst it is an observational fact, only a snapshot at a specific time can be captured. Conversely, numerical simulations can detail these characteristics three-dimensionally, including temporal evolution, thereby significantly advancing meteorological and physical interpretation. From this perspective, it becomes possible to elucidate not only the correlation itself but also the underlying physical processes driving it. Unlike bulk methods constrained by drop-size distributions, this approach allows pure characterisation of cloud microphysical responses to environmental conditions across diverse scenarios.

The aim of this study is to investigate relationships between cloud microphysical processes and their response to the environmental conditions of the surrounding atmosphere, as provided by the initial profile, including the underlying physical processes. Section 2 describes experimental design used in this study. The main results are described in Sect. 3, divided into four subsections: Section 3.1 gives horizontal structures of the simulated convective clouds obtained in this study, Section 3.2 shows the rainfall statistics, as well as in-cloud properties of the systems in Sect. 3.3, and the vertical profiles of drop-size distribution within the systems in Sect. 3.4, respectively. In Sect. 4, responses from environmental condition to in-cloud properties and implication for QPE are discussed. Finally, Section 5 describes summary of the main results in this study.

https://doi.org/10.5194/egusphere-2026-1725
Preprint. Discussion started: 27 April 2026

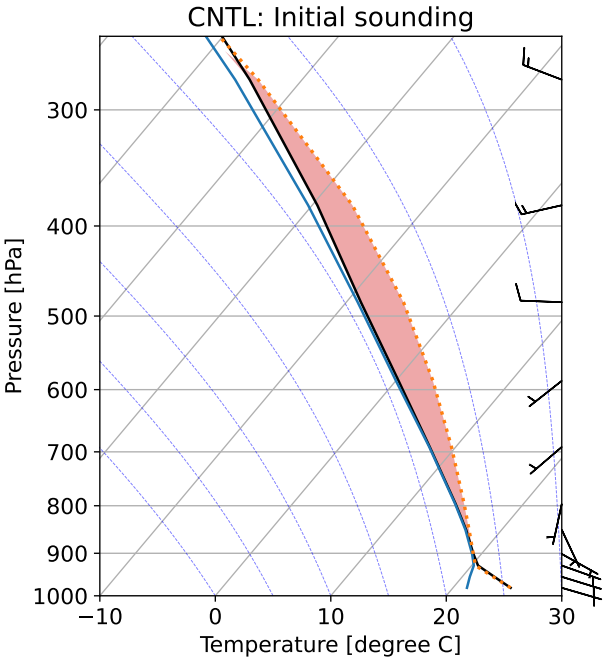

Figure 1. Skew T–log$p$ diagrams of the initial condition for CONTROL (CNTL) experiment on this study.

2 Experimental design

2.1 Numerical setup

The cloud-resolving numerical model used was version 4.5.2 of the Advanced Research for Weather Research and Forecasting model (Skamarock et al., 2019). The computational domain was set to 80 km × 80 km horizontally and 20 km vertically. The horizontal grid spacing was set to 250 m, and the vertical grid spacing was set to achieve an average of 140 m. As boundary conditions, a Rayleigh damping layer was set at 7 km from the top to suppress the reflection of gravity waves by convection. The lower boundary was set to no friction. Side boundaries were treated as radiative. To focus on the dynamics of individual convection cells, the physical processes were simplified to include only cloud microphysical processes and boundary-layer turbulence. For cloud microphysics, the Spectrum bin scheme developed at the Hebrew University (hereafter WRF-SBM) was used (Shpund et al., 2019). For the boundary-layer turbulence process, (Deardorff, 1980) scheme, which solves the turbulence energy at 1.5th order, was used. The Coriolis force was neglected. Initial conditions were based on a heavy-rain-produced convective cloud case investigated by (Unuma et al., 2023). An initial sounding data near Kumagaya was created from Japan Meteorological Agency's Mesoscale Model and applied uniformly horizontally (Fig. 1).

https://doi.org/10.5194/egusphere-2026-1725
Preprint. Discussion started: 27 April 2026

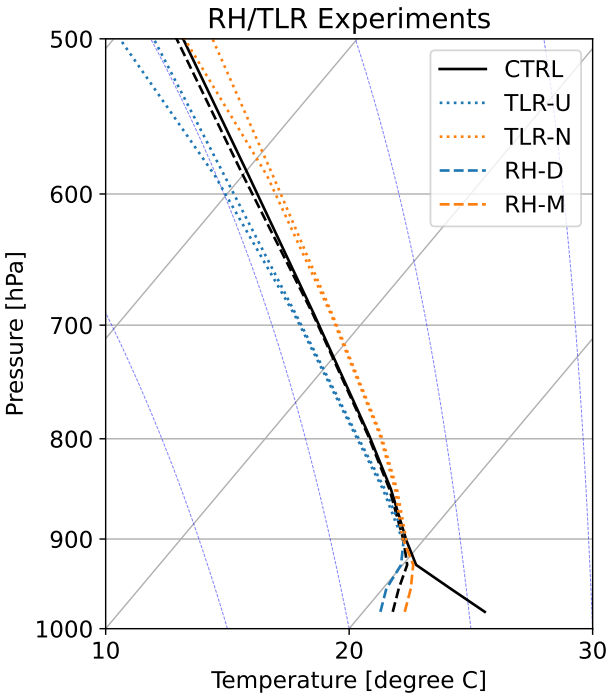

Figure 2. As is Fig. 1, but for RH and TLR experiments.

2.2 Sensitivity experiments

Based on observational relationships obtained in Unuma (2025). Specifically, these experiments included: increasing or decreasing the relative humidity in the layer below the lifting condensation level by up to 2 % (RH experiment); changing the temperature lapse rate in the layer above the lifting condensation level by up to 2 K km^{-1} (TLR experiment); and varying the wind speed throughout the troposphere to 0.5 or 1.5 times its original value (SH experiment). The TLR experiment was conducted primarily because there is a positive correlation between the height of the temperature lapse rate and the drop size within convective clouds. Numerical experiments (e.g., Houston and Niyogi, 2007; Takemi, 2007; Sueki, 2024) have been conducted with similar assumptions. The RH experiment was conducted primarily because there is a positive correlation between water vapor content near the surface and rainfall. Numerical experiments (e.g., Kato et al., 2003; Schumacher, 2015) have been performed under similar assumptions. The SH experiment was conducted primarily because there is a positive (negative) correlation between the magnitude of the vertical shear of the horizontal wind within the troposphere and the drop size (number concentration). Here, to vary the magnitude of vertical shear, both east-west and north-south winds were changed simultaneously. Since altering the hodograph shape was found to affect the temporal evolution of the original convective cloud significantly, we decided not to change the hodograph shape this time and varied only the magnitude of the shear.

https://doi.org/10.5194/egusphere-2026-1725
Preprint. Discussion started: 27 April 2026

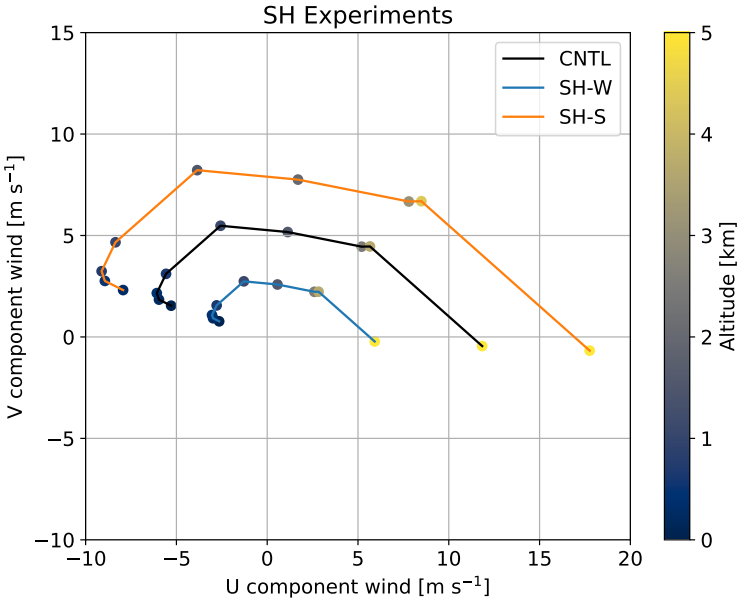

Figure 3. Hodographs for CNTL, weaker vertical wind shear (SH-W), and stronger vertical wind shear (SH-S) experiments.

2.3 DSD parameters for raindrops

In WRF-SBM, number concentration ($\#$ kg kg^{-1}) in each bin can be archived with the output variables of `ff1i`nn (nn is ranging from 01 to 33), where 01–16 bins represent cloud category and 17–33 bins represent rain category, respectively. To obtain drop-size distribution ($n(D)$) from the `ff1i`nn variables, $n(D)$ is calculated as

$$n(D) = \frac{\texttt{ff1i}(D)}{M_{\mathrm{cloud,rain}}(D)} \frac{\rho_{\mathrm{cloud,rain}}(D)}{\Delta D}, \tag{1}$$

where `ff1i`(D) is equivalent to `ff1inn` but bin diameter D (mm) oriented expression, $M_{\mathrm{cloud,rain}}(D)$ is the mass of liquid drops (kg), $\rho_{\mathrm{cloud,rain}}(D)$ is the density of liquid drops for dry air (kg m^{-3}), and ΔD is the drop-size spread (mm) in diameters, respectively. For the retrieval of DSD parameters on raindrops, i.e., the mass-weighted volume diameter (D_{m}; mm), the generalised intercept parameter (N_{w}; mm^{-1} m^{-3}), the liquid water content (LWC; g m^{-3}), were calculated assuming the normalised gamma distribution based on a momentum technique (Hardin and Guy, 2017) as following procedures. The normalised gamma distribution (e.g., Testud et al., 2001) is expressed as follows;

$$N(D) = N_{\mathrm{w}} f(\mu) \left(\frac{D}{D_{\mathrm{m}}} \right)^{\mu} \exp \left[-(4+\mu) \frac{D}{D_{\mathrm{m}}} \right], \tag{2}$$

where N_{w} and $f(\mu)$ are defined as

https://doi.org/10.5194/egusphere-2026-1725
Preprint. Discussion started: 27 April 2026

$$N_{\mathrm{w}} = \frac{4^4 \mathrm{LWC}}{\pi \rho_{\mathrm{w}} D_{\mathrm{m}}^4}, \tag{3}$$

and

$$f(\mu) = \frac{\Gamma(4)}{4^4} \frac{(4+\mu)^{(4+\mu)}}{\Gamma(4+\mu)}. \tag{4}$$

Here, μ is a shape parameter, ρ_{w} is the density of water ($\mathrm{g\ m^{-3}}$), and Γ is the Gamma function. LWC and D_{m} are obtained from the following equations;

$$\mathrm{LWC} = \frac{\pi \rho_{\mathrm{w}}}{6} \sum_{i=17}^{33} n(D_i) D_i^3, \tag{5}$$

and

$$D_{\mathrm{m}} = \frac{\sum_{i=17}^{33} n(D_i) D_i^4}{\sum_{i=17}^{33} n(D_i) D_i^3}. \tag{6}$$

The bin ranges from 17 to 33 were selected for retrieving the parameters because the parameters were envisaged to raindrops. Rainfall intensity R ($\mathrm{mm\ h^{-1}}$) is calculated from the simulated DSD data with the following equation:

$$R = 6 \times 10^{-4} \pi \sum_{i=17}^{33} n(D_i) V(D_i) D_i^3. \tag{7}$$

When the R calculation, the data within $\pm$ 50 % of the raindrop-fall velocity formula of Atlas et al. (1973) are used.

2.4 Identification and tracking of simulated convective clouds

Individual convective clouds were detected and tracked using *tobac* algorithm version 1.5.5 (Sokolowsky et al., 2024) as in Unuma (2025). *tobac* algorithm identifies peak positions in the region above or below a specified threshold value at each time step, referred to as a 'feature'. The area occupied by this feature is determined through a process called 'segmentation', which utilises a water shedding algorithm (Carpenter et al., 2006; van der Walt et al., 2014) to establish boundaries both horizontally and vertically. A set of features is tracked over time using the method described by Crocker and Grier (1996). Each feature or group of features is defined as a 'cell', with the path it follows referred to as a 'track', assessed in three dimensions. In this study, cells were used for the analysis the distinct characteristics of convective clouds that resulted in heavy rainfall at the model surface.

https://doi.org/10.5194/egusphere-2026-1725
Preprint. Discussion started: 27 April 2026

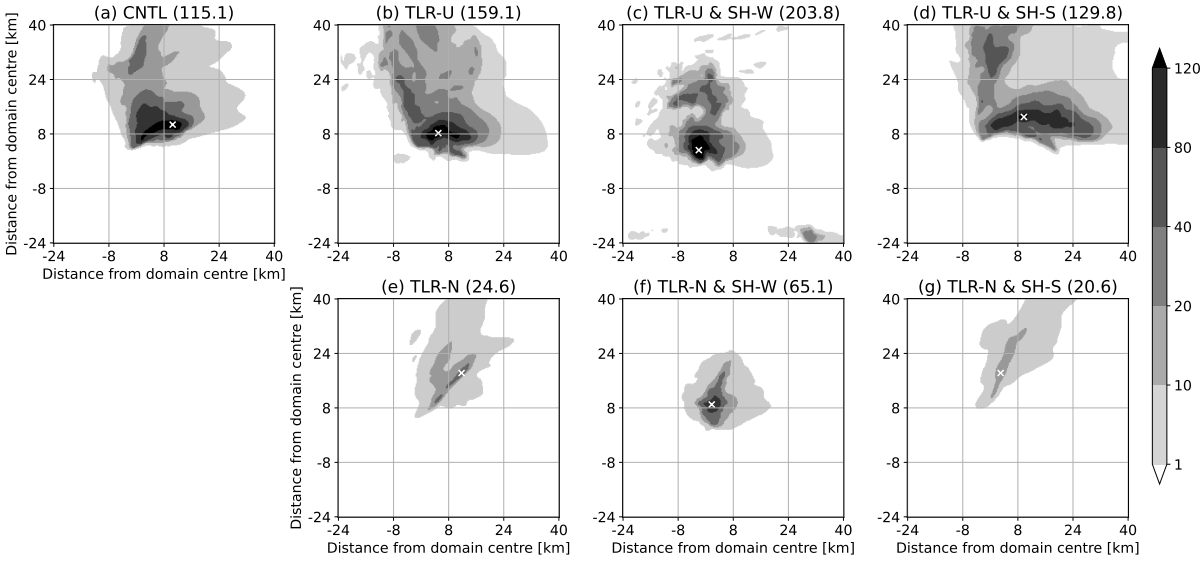

Figure 4. Horizontal distribution of 2-hour accumulated rainfall for CNTL, TLR-N, TLR-U, TLR-N & SH-W, TLR-U & SH-W, TLR-N & SH-S, and TLR-U & SH-S experiments. White crosses displayed in each panel are the point where the maximum value of the accumulated rainfall simulated.

3 Results

3.1 Horizontal structures of simulated convective clouds with the environmental sensitivities

Figure 4 shows the horizontal distribution of the accumulated rainfall for the calculation period. The maximum value of the accumulated rainfall increases by 38 % when the temperature lapse rate is high (TLR-U), whilst it decreases by 79 % when the temperature lapse rate is low (TLR-N). The rainfall area expands slightly northward with higher temperature lapse rates (TLR-U), but shrinks significantly at lower temperature lapse rates (TLR-N). The effect of vertical shear under high-temperature lapse-rate conditions were also examined. The rainfall area was larger when the vertical shear was strong (Fig. 4d). When vertical shear was weak (Fig. 4f), the maximum rainfall tended to occur farther southwest than in CNTL experiment. Notably, when the temperature lapse rate was high and vertical wind shear was weak, the accumulated rainfall shows highest value among the TLR experiments, and the rainfall area was narrower than the stronger shear case.

When the relative humidity in the lower troposphere is low (RH-D), the maximum value of the accumulated rainfall decreases by 23 % (Fig. 5e). In comparison, it increases by 62 % (Fig. 5b) when the relative humidity is high (RH-M). The rainfall area remains largely unchanged, though it shows a slight tendency to decrease when the lower-troposphere relative humidity (RH-M) is high. The effect of vertical shear was confirmed when lower-troposphere relative humidity was low. In both cases, the maximum value of the accumulated rainfall was lower compared to CNTL experiment; however, the rate of decrease is higher when vertical wind shear is strong (SH-S) and lower when it is weak (SH-W). The location where the peak value occurs

https://doi.org/10.5194/egusphere-2026-1725
Preprint. Discussion started: 27 April 2026

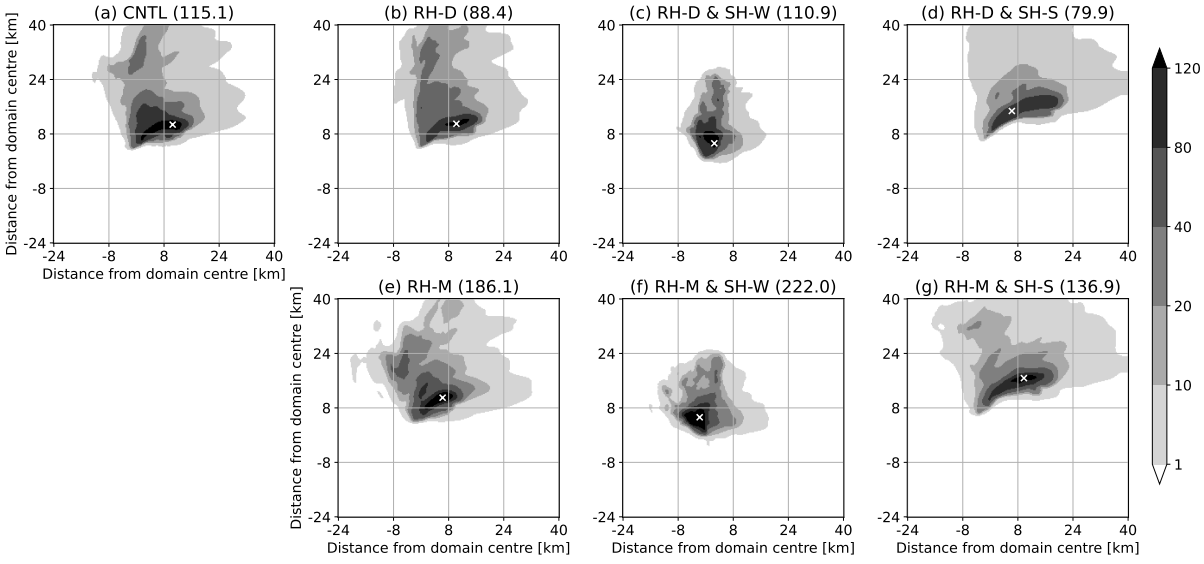

Figure 5. As in 4, but for RH experiments.

was also slightly biased southwestward compared to when the vertical wind shear is weak (SH-W), and the rainfall area is significantly narrow. This trend is quiet similar to TLR experiments.

3.2 Rainfall statistics

Figure 6 shows the time series of the maximum rainfall intensity within the domain. The temperature lapse rate of the surrounding atmosphere directly influenced rainfall intensity. Specifically, when the temperature lapse rate was low (TLR-U), rainfall intensity tended to reach higher maximum values compared to CNTL. The strength of vertical shear acts in a direction that increases rainfall intensity. On the other hand, when the temperature lapse rate is high and close to neutral (TLR-N), the onset of rainfall intensity is generally delayed, and the intensity itself is smaller. Notably, the maximum rainfall intensity decreases with increasing vertical shear strength, unlike other trends.

Similarly, the cases of low-level moisture are shown (Fig. 7). Overall, the maximum rainfall intensity increases sharply around 30 min after the start of the calculation, whilst no extreme fluctuations occur after 50 min. In cases of strong shear (RH-D & SH-S and RH-M & SH-S), the rise in rainfall intensity was faster, and the maximum rainfall intensity was larger compared to the CNTL experiment. However, these intensities tended to be stronger when the lower troposphere was moist. When vertical shear was weak, the onset of rainfall intensity was delayed, and the maximum rainfall intensity was lower than in the CNTL experiment. In this scenario, the maximum rainfall intensity decreased as the moisture content in the lower troposphere decreased.

To gain a more quantitative understanding of the horizontal distribution trends shown in the previous section, the maximum rainfall intensity and the domain statistics of accumulated rainfall were examined. Figure 8a shows a box plot of the maximum

https://doi.org/10.5194/egusphere-2026-1725
Preprint. Discussion started: 27 April 2026

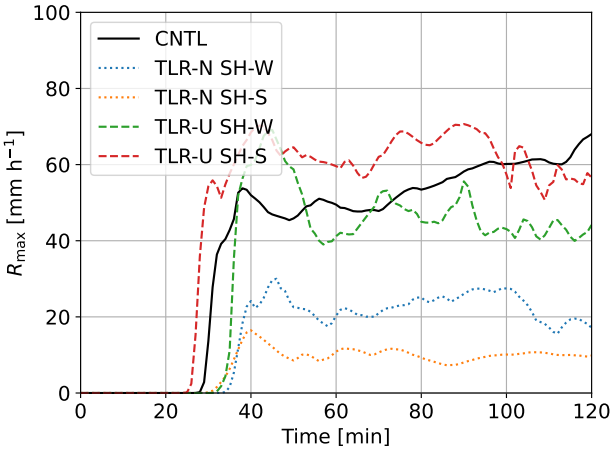

Figure 6. Time series of the rainfall intensity maxima ($R_{\max}$; mm h^{-1}) within the domain for TLR and SH experiments.

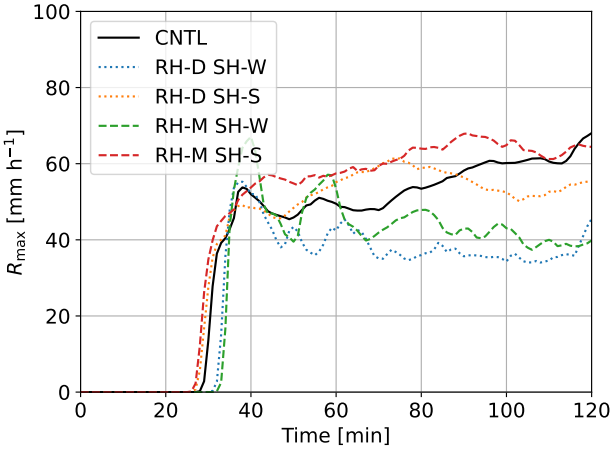

Figure 7. As in 6, but for RH and SH experiments.

rainfall intensity within the computational domain. The maximum rainfall intensity tends to increase with higher relative humidity in the lower troposphere and stronger vertical shear, as well as with a higher temperature lapse rate and stronger vertical shear. Conversely, when relative humidity is low and vertical shear is weak, the maximum rainfall intensity tends to decrease. However, this trend does not hold when the temperature lapse rate is low. In fact, the maximum rainfall intensity tends to be higher when the vertical shear is weak than when it is strong. Nevertheless, these values are smaller than those observed in CNTL experiment.

Figure 8b shows the box-and-whisker plot of the total rainfall within the computational domain. In contrast to the maximum rainfall intensity mentioned above, accumulated rainfall maximum tends to be higher when vertical shear is weak, except when the temperature lapse rate is high. When the temperature lapse rate is high, accumulated rainfall maximum tends to be higher

https://doi.org/10.5194/egusphere-2026-1725
Preprint. Discussion started: 27 April 2026

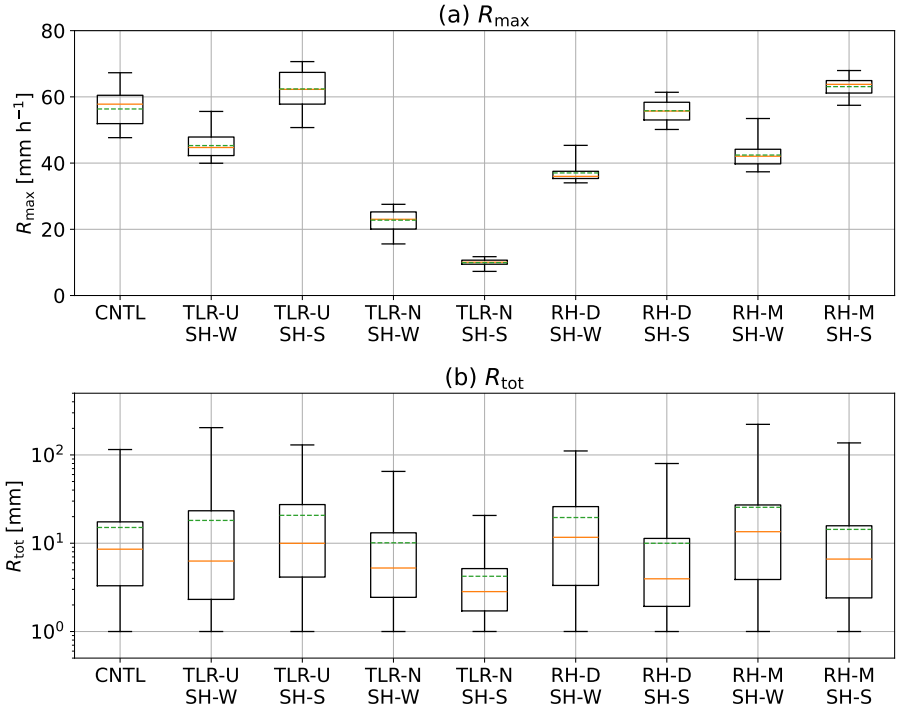

Figure 8. Box-whisker plots of the maximum value of rainfall intensity ($R_{\max}$; $\mathrm{mm\ h^{-1}}$, upper panel) and the maximum accumulated rainfall (R_{tot}; mm, lower panel) in $\log_{10}$ scale among the experiments. The box extends 25th and 75th percentile values with orange and green lines at the median and mean values, respectively.

with strong vertical shear. However, as confirmed in the horizontal distribution, the maximum value is larger when the vertical shear is weak. In the horizontal distribution, the spread of total rainfall increases with stronger vertical shear, suggesting that the statistical value tends to be higher. The response to vertical flow is not particularly large for humidity, but it is sensitive to temperature lapse rates and vertical wind shear. How do these differences manifest within convective clouds? Cases with the rainfall intensity maxima (i.e., TLR-U & SH-S) to those with the accumulated rainfall maxima (i.e., RH-M & SH-W) were compared in the following subsection.

3.3 In-cloud properties: DSD parameters

Figure 9 detects and tracks the most developed convective cloud within the computational domain, showing a time-altitude profile near its centre limited to the period around the peak time. In the TLR-U & SH-S experiment, which produced the maximum rainfall intensity, drop sizes with a mass-weighted mean diameter of 3.0 mm or larger were dominant (Fig. 9a), and areas with high number concentrations corresponded to regions with a mass-weighted mean diameter around 3.0 mm (Fig. 9c). In contrast, in the RH-M & SH-W experiment, which produced the maximum accumulated rainfall, raindrops with a mass-weighted mean diameter of 2.0–3.0 mm were dominant (Fig. 9b), with a particularly high number concentration for

https://doi.org/10.5194/egusphere-2026-1725
Preprint. Discussion started: 27 April 2026

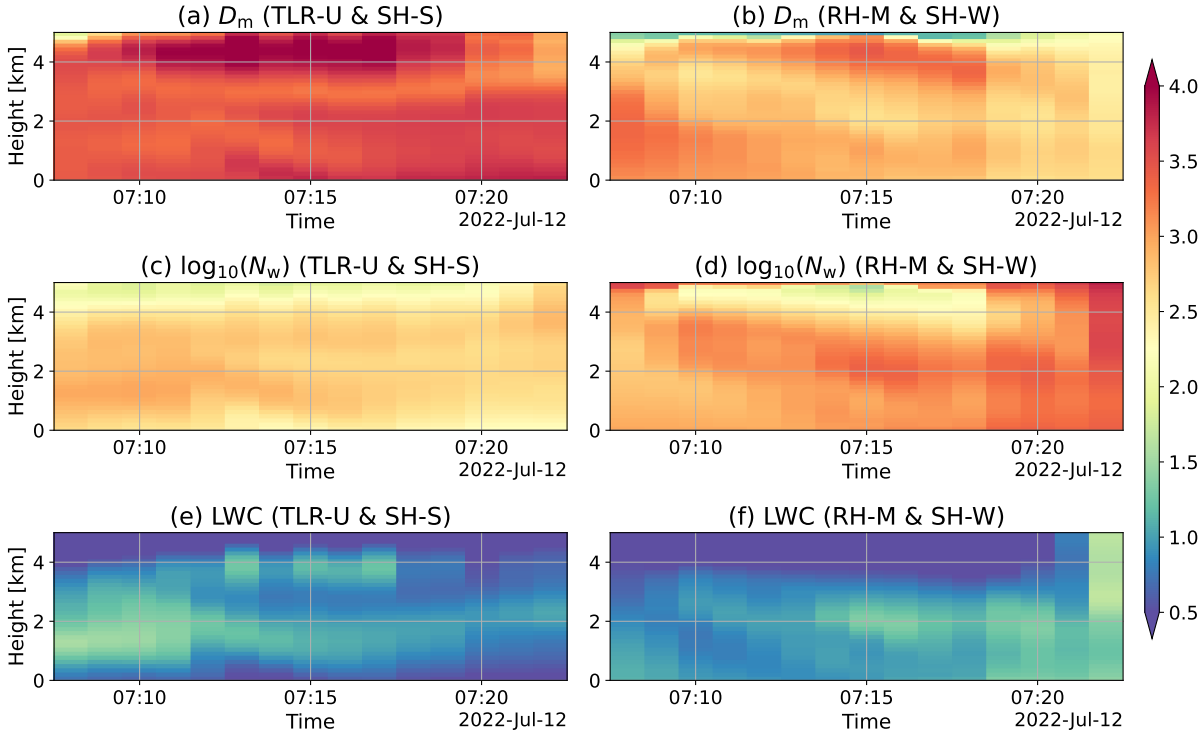

Figure 9. Time-height sections of the DSD parameters near the convective cloud centre. The left column shows the right column shows the TLR-U & SH-S experiment, and the RH-W & SH-W experiment, the centre column shows the CNTL experiment. The top row shows the mass-weighted mean diameter (D_m; mm), the middle row shows the generalised intercept parameter (N_w; $\mathrm{mm}^{-1}\ \mathrm{m}^{-3}$) in $\log_{10}$ scale, and the bottom row shows liquid water content (LWC; $\mathrm{g\ m}^{-3}$). These DSD parameters were calculated using a moment-based method.

mass-weighted mean diameter of 2.0 mm (Fig. 9d). Areas with high rainfall amounts similarly corresponded primarily to these high number concentrations. These results indicate that, when rainfall intensity is maximised, the mass-weighted mean diameter directly contributes to the rainfall amount within the convective cloud (e.g., Fig. 9e). Conversely, when total rainfall is maximised, although the mass-weighted mean diameter is 2.0 mm, the high number concentration contributes to rainfall within the convective cloud (e.g., Fig. 9f).

3.4 Vertical profiles of drop-size distribution

The calculation of drop-size distribution parameters is fundamentally based on raindrops (c.f., Sect. 2.3) and thus does not include information on cloud droplets. The conversion process of cloud droplets to raindrops and the interactions between cloud and raindrops are important; however, direct observation is difficult due to instrument limitations (e.g., Unuma, 2025). Here, we aim to understand the drop-size distribution, including cloud droplets, in situations where spectral-bin cloud microphysical processes may occur within the resolvable range. Figure 10 shows the vertical profile of the drop size-distribution at the

https://doi.org/10.5194/egusphere-2026-1725
Preprint. Discussion started: 27 April 2026

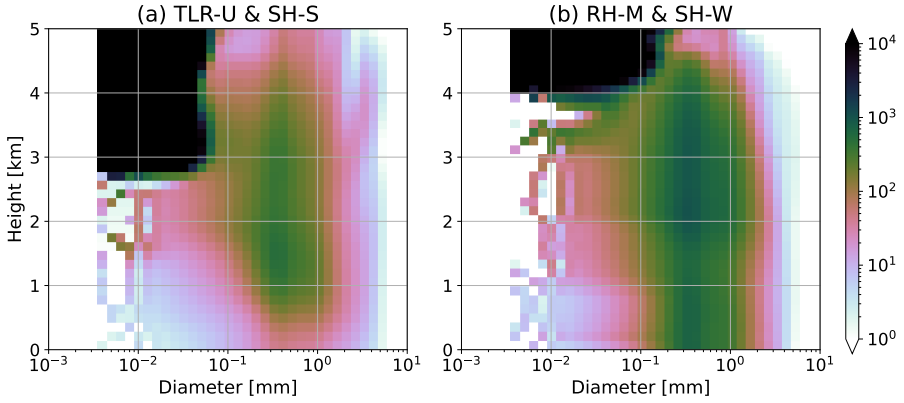

Figure 10. Two-dimensional histograms of the vertical profile of drop-size distribution ($\mathrm{mm}^{-1}\ \mathrm{m}^{-3}$) on cloud and rain categories obtained from WRF-SBM simulations using Eq. (1) in the experiment of TLR-U & SH-S (left) and RH-M & SH-W (right).

peak time for the convective clouds detected and tracked as shown in Fig. 9, presented as a two-dimensional histogram. For cases with maximum accumulated rainfall, within the size range of 0.2–1 mm and below an altitude of 4 km, the vertical variation in number concentration is small, indicating high vertical uniformity. In contrast, when rainfall intensity is maximum, within the 0.2–1 mm drop size range and at altitudes below 4 km, the vertical variation in number concentration is large. Between 4 and 1 km altitude, the number concentration increases toward the surface, whereas below 1 km altitude, it is low. In summary, within the range of raindrop size distribution, when an accumulated rainfall is maximised, vertical variation in raindrop size distribution is small at its peak. However, when a rainfall intensity is maximised, vertical variation in the raindrop size distribution is large, and particularly near the surface, its shape differs significantly from that at higher altitudes. What about cloud droplets? When an accumulated rainfall is maximised, droplet number concentration is very high above 4 km altitude, but below that level it decreases gradually toward the ground within the 0.01–0.1 mm size range. When a rainfall intensity is at its maximum, cloud droplet number concentration is very high above 3 km altitude. Below this level, however, the number concentration decreases sharply toward the surface. This rate of decrease is particularly pronounced below 1 km altitude compared to when the accumulated rainfall is at its maximum.

4 Discussion

4.1 Responses from environments to in-cloud properties

Unuma (2025) showed that drop size tends to increase under conditions of higher temperature lapse rate and stronger vertical shear, whilst number concentration tends to increase under conditions of higher moisture content in the lower troposphere and weaker vertical shear. Whilst these results were based on observational data, they did not delve into the underlying physical processes. The results of this study indicate that the temperature lapse rate fundamentally controls the peak rainfall intensity.

https://doi.org/10.5194/egusphere-2026-1725
Preprint. Discussion started: 27 April 2026

At the same time, vertical shear is sensitive to the time required for rainfall intensity to reach its peak and to its maximum intensity. Conversely, when the lower troposphere is highly moist, sensitivity to the speed of convective clouds is observed. Furthermore, the strength of vertical shear can control both the speed of convective cloud motion and its maximum intensity. Specifically, as shown in the rainfall intensity time series for temperature lapse rate (Fig. 6) and maximum intensity (Fig. 8a), the maximum rainfall intensity tends to be greater when the lapse rate value is larger (i.e., more unstable) and when vertical shear is stronger. This result is also reflected in the drop-size distribution parameters, where it fundamentally increases the D_{m} value (Fig. 9), thereby contributing to the rainfall intensity, as reflected in its integral value. Additionally, regarding the vertical profile of the drop-size distribution, its variation becomes larger, characterised particularly by a greater proportion of evaporative cooling of raindrops near the ground. On the other hand, the maximum intensity is not as strongly affected by lower-tropospheric humidity as by the temperature lapse rate (Fig. 7). Rather, the maximum rainfall intensity tends to be controlled by the strength of the vertical shear (Fig. 8a). This feature is resembled to the previous study (e.g., Li and Xue, 2026). Regarding the characteristics of drop size distribution parameters, the height of N_{w} generally increases with rainfall intensity (Fig. 9). Notably, the vertical profile of the drop-size distribution shows little significant change (Fig. 10). This result suggests that collisional coalescence and collisional breakup between raindrops may dominate over evaporative cooling (e.g., Paukert et al., 2019), potentially forming a stationary distribution (e.g., Low and List, 1982; McFarquhar, 2004; Unuma et al., 2025).

4.2 Implications for quantitative precipitation estimation

When the drop size distribution does not change vertically, the impact of evaporation may not warrant much weight. Conversely, when vertical shear or temperature lapse rates increase, vertical variability must be factored in, generally requiring downward adjustments. For radar QPE at least in Japan, adjustments are sometimes made through rain gauge data, but vertical variability itself is rarely considered for now, which could provide valuable insights. How much adjustment is needed depending on environmental conditions? For example, in the absence of interaction with the surrounding atmosphere, in a vertically one-dimensional context, the model depends heavily on the given humidity profile, and the spread of the drop-size distribution toward larger sizes—i.e., the spectral width—is readily constrained. Extending this to three dimensions, as in this study, incorporates horizontal advection in addition to vertical advection and evaporation. The effect of horizontal advection is thought to depend on the magnitude of the vertical shear of the horizontal wind and is expected to promote collisional coalescence between raindrops. Consequently, it is expected to broaden the spectral width whilst reducing the number concentration of small droplets. This results in an increase in D_{m} and a decrease in N_{w} as parameters of the drop-size distribution. Conversely, in environments with high relative humidity and weak vertical wind shear, evaporation is less likely, but the rate of collisional coalescence between raindrops is expected to decrease. Consequently, whilst the spectral width remains narrow, the number concentration on the small-diameter side is expected to increase. These results lead to the opposite effect from the previous case: D_{m} decreases, whilst N_{w} increases.

https://doi.org/10.5194/egusphere-2026-1725
Preprint. Discussion started: 27 April 2026

5 Conclusions

Environmental conditions play a significant role in the intensity of organised convective systems. However, variations in factors such as temperature, humidity, and vertical wind shear indicate that non-linear relationships may exist between these systems and their environments. To address the gaps in understanding these variations, it is essential to examine the microphysical processes within convective systems. In this study, we conducted numerical experiments using the Weather Research and Forecasting model with idealised setups that included a spectral-bin microphysical scheme to treat drop-size distributions explicitly. The initial conditions varied in humidity, temperature lapse rates, and vertical wind shear, reflecting observed relationships between environmental conditions and drop-size distribution parameters based on (Unuma, 2025).

Our results indicated that larger temperature lapse rates led to larger raindrops, resulting in more intense rainfall. Additionally, increased moisture in the lower troposphere generated stronger rainfall intensity, driven by a higher concentration of smaller raindrops and greater liquid water content. The magnitude of vertical wind shear generally causes fluctuations in the drop size distribution within convective clouds. Specifically, weaker vertical shear tends to inhibit the propagation of convective clouds, reduce vertical variations in the drop size distribution within them, and decrease the raindrop evaporation rate, ultimately increasing rainfall amounts.

In particular, we found differences in the vertical profiles of particle size distributions within convective clouds between cases with maximum rainfall intensity and those with maximum accumulated rainfall. We found that when rainfall intensity is maximum, the vertical variation in the drop-size distribution is large (particularly near the ground surface). In contrast, when accumulated rainfall is maximum, the vertical variation in the drop-size distribution is smaller, at least below the melting layer. The former is probably due to the ease with which cloud droplets and small raindrops evaporate, which is consistent with previous studies (e.g., Xie et al., 2016). In contrast, the latter is likely to occur when the evaporation rates of cloud droplets and small raindrops are lower than in the former case. It has been pointed out that in convective systems producing heavy rain, processes such as collisional coalescence and collisional breakup between raindrops become dominant over evaporative cooling (e.g., Paukert et al., 2019), and in such cases, the drop-size distribution is interpreted as being an equilibrium shape (e.g., Low and List, 1982).

However, whilst convective clouds that produce heavy rain are expected to interact with the surrounding atmosphere, few studies have investigated the dominant cloud microphysical processes by extending these interactions to the drop-size distribution within the convective clouds. This fact is simply because observational data, even when available, are merely snapshots, making it difficult to establish causal relationships. In this regard, this study succeeded in deciphering signals derived from limited observational data and, by analysing these relationships, obtained results that shed light on the underlying physical processes—albeit under idealised conditions. It has the potential to serve as a pioneering study that bridges mesoscale and microscale processes in meteorology. In this context, it significantly improves QPE and refines the physical processes handled in microphysics schemes within numerical modelling.

https://doi.org/10.5194/egusphere-2026-1725
Preprint. Discussion started: 27 April 2026

Code availability. WRF codes used in this study are available on GitHub at https://github.com/wrf-model/WRF/releases/tag/v4.5.2 (last access: 24 March 2026).

Data availability. Input sounding data used in this study are available upon request from the corresponding author.

Author contributions. The author confirms sole responsibility for the study conception and design, data collection, analysis and interpretation of results, and manuscript preparation.

Competing interests. The author declares that there are no competing interests.

Acknowledgements. This research has been supported by the Japan Society for the Promotion of Science (grant no. JP24K17126) and Initiative on Recommendation Program for Young Researchers and Woman Researchers, Information Technology Center, The University of Tokyo.

https://doi.org/10.5194/egusphere-2026-1725
Preprint. Discussion started: 27 April 2026

References

Atlas, D., Srivastava, R. C., and Sekhon, R. S.: Doppler radar characteristics of precipitation at vertical incidence, Rev. Geophys., 11, 1–35, https://doi.org/10.1029/RG011i001p00001, 1973.

Bringi, V. N., Chandrasekar, V., Hubbert, J., Gorgucci, E., Randeu, W. L., and Schoenhuber, M.: Raindrop size distribution in different climatic regimes from disdrometer and dual-polarized radar analysis, J. Atmos. Sci., 60, 354–365, https://doi.org/10.1175/1520-0469(2003)060<0354:RSDIDC>2.0.CO;2, 2003.

Carpenter, A. E., Jones, T. R., Lamprecht, M. R., Clarke, C., Kang, I. H., Friman, O., Guertin, D. A., Chang, J. H., Lindquist, R. A., Moffat, J., Golland, P., and Sabatini, D. M.: CellProfiler: image analysis software for identifying and quantifying cell phenotypes, Genome Biology, 7, https://doi.org/10.1186/gb-2006-7-10-r100, 2006.

Crocker, J. C. and Grier, D. G.: Methods of digital video microscopy for colloidal studies, Journal of Colloid and Interface Science, 179, 298–310, https://doi.org/10.1006/jcis.1996.0217, 1996.

Deardorff, J. W.: Stratocumulus-capped mixed layers derived from a three-dimensional model, Bound.-Lay. Meteorol., 18, 495–527, https://doi.org/10.1007/bf00119502, 1980.

Diehl, K., Jungbluth, T., Theis, A., Mitra, S. K., and Szakáll, M.: Wind tunnel experiments of spontaneous and collision-induced breakup of raindrops and model simulations of the impact of breakup on precipitation, Atmos. Res., p. 108327, https://doi.org/https://doi.org/10.1016/j.atmosres.2025.108327, 2025.

Ding, J., Tian, W., Xiao, H., Cheng, B., Liu, L., Sha, X., Song, C., Sun, Y., and Shu, W.: Raindrop size distribution and microphysical features of the extremely severe rainstorm on 20 July 2021 in Zhengzhou, China, Atmos. Res., 289, 106 739, https://doi.org/10.1016/j.atmosres.2023.106739, 2023.

Dolan, B., Fuchs, B., Rutledge, S. A., Barnes, E. A., and Thompson, E. J.: Primary modes of global drop size distributions, J. Atmos. Sci., 75, 1453–1476, https://doi.org/10.1175/JAS-D-17-0242.1, 2018.

Gupta, A. K., Deshmukh, A., Waman, D., Patade, S., Jadav, A., Phillips, V. T. J., Bansemer, A., Martins, J. A., and Gonçalves, F. L. T.: The microphysics of the warm-rain and ice crystal processes of precipitation in simulated continental convective storms, Comm. Earth and Environ., 4, https://doi.org/10.1038/s43247-023-00884-5, 2023.

Hardin, J. and Guy, N.: PyDisdrometer v1.0, Zenodo [code], https://doi.org/10.5281/zenodo.9991, 2017.

Houston, A. L. and Niyogi, D.: The Sensitivity of Convective Initiation to the Lapse Rate of the Active Cloud-Bearing Layer, Mon. Weather Rev., 135, 3013–3032, https://doi.org/10.1175/MWR3449.1, 2007.

Hu, Z. and Srivastava, R. C.: Evolution of raindrop size distribution by coalescence, breakup, and evaporation: Theory and observations, J. Atmos. Sci., 52, 1761–1783, https://doi.org/10.1175/1520-0469(1995)052<1761:EORSDB>2.0.CO;2, 1995.

James, R. P., Markowski, P. M., and Fritsch, J. M.: Bow echo sensitivity to ambient moisture and cold pool strength, Mon. Weather Rev., 134, 950–964, https://doi.org/10.1175/MWR3109.1, 2006.

Johnson, R. H., Rickenbach, T. M., Rutledge, S. A., Ciesielski, P. E., and Schubert, W. H.: Trimodal characteristics of tropical convection, J. Climate, 12, 2397–2418, https://doi.org/10.1175/1520-0442(1999)012<2397:TCOTC>2.0.CO;2, 1999.

Kato, T.: Quasi-stationary band-shaped precipitation systems, named "Senjo-Kousuitai", causing localized heavy rainfall in Japan, J. Meteorol. Soc. Japan, 98, 485–509, https://doi.org/10.2151/jmsj.2020-029, 2020.

https://doi.org/10.5194/egusphere-2026-1725
Preprint. Discussion started: 27 April 2026

Kato, T., Yoshizaki, M., Bessho, K., Inoue, T., Sato, Y., and observation group, X.-B.-.: Reason for the failure of the simulation of heavy rainfall during X-BAIU-01–Importance of a vertical profile of water vapor for numerical simulations–, J. Meteorol. Soc. Japan, 81, 993–1013, https://doi.org/10.2151/jmsj.81.993, 2003.

Kikuchi, K. and Takayabu, Y. N.: The development of organized convection associated with the MJO during TOGA COARE IOP: Trimodal characteristics, Geophys. Res. Lett., 31, https://doi.org/https://doi.org/10.1029/2004GL019601, 2004.

Kumjian, M. R., Khain, A. P., Benmoshe, N., Ilotoviz, E., Ryzhkov, A. V., and Phillips, V. T. J.: The anatomy and physics of Z_{DR} columns: Investigating a polarimetric radar signature with a spectral bin microphysical model, J. Appl. Meteorol. Climat., 53, 1820–1843, https://doi.org/10.1175/JAMC-D-13-0354.1, 2014.

Li, J. and Xue, M.: Strong sensitivity of simulated supercells to low-level moisture: Effects of near-cloud-base moisture entrainment, J. Atmos. Sci., 83, 125–150, https://doi.org/10.1175/jas-d-24-0272.1, 2026.

Li, M., Zhang, F., Zhang, Q., Harrington, J. Y., and Kumjian, M. R.: Nonlinear response of hail precipitation rate to environmental moisture content: A real case modeling study of an episodic midlatitude severe convective event, J. Geophys. Res.-Atmos, 122, 6729–6747, https://doi.org/10.1002/2016JD026373, 2017.

Li, X. and Srivastava, R. C.: An analytical solution for raindrop evaporation and its application to radar rainfall measurements, Journal of Applied Meteorology, 40, 1607–1616, https://doi.org/10.1175/1520-0450(2001)040<1607:AASFRE>2.0.CO;2, 2001.

Low, T. B. and List, R.: Collision, coalescence and breakup of raindrops. Part I: Experimentally established coalescence efficiencies and fragment size distributions in breakup, J. Atmos. Sci., 39, 1591–1606, https://doi.org/10.1175/1520-0469(1982)039<1591:CCABOR>2.0.CO;2, 1982.

Lucas, C., Zipser, E. J., and Lemone, M. A.: Vertical velocity in oceanic convection off tropical Australia, J. Atmos. Sci., 51, 3183–3193, https://doi.org/10.1175/1520-0469(1994)051<3183:VVIOCO>2.0.CO;2, 1994.

McFarquhar, G. M.: A new representation of collision-induced breakup of raindrops and its implications for the shapes of raindrop size distributions, J. Atmos. Sci., 61, 777–794, https://doi.org/10.1175/1520-0469(2004)061<0777:ANROCB>2.0.CO;2, 2004.

Morrison, H., Tessendorf, S. A., Ikeda, K., and Thompson, G.: Sensitivity of a simulated midlatitude squall line to parameterization of raindrop breakup, Mon. Weather Rev., 140, 2437–2460, https://doi.org/10.1175/MWR-D-11-00283.1, 2012.

Morrison, H., Morales, A., and Villanueva-Birriel, C.: Concurrent sensitivities of an idealized deep convective storm to parameterization of microphysics, horizontal grid resolution, and environmental static stability, Mon. Weather Rev., 143, 2082–2104, https://doi.org/10.1175/MWR-D-14-00271.1, 2015.

Nagata, K.: Quantitative precipitation estimation and quantitative precipitation forecasting by the Japan Meteorological Agency, RSMC Tokyo-Typhoon Center Tech. Rev., 13, 37–50, https://www.jma.go.jp/jma/jma-eng/jma-center/rsmc-hp-pubeg/techrev/text13-2.pdf, 2011.

Paukert, M., Fan, J., Rasch, P. J., Morrison, H., Milbrandt, J. A., Shpund, J., and Khain, A.: Three-moment representation of rain in a bulk microphysics model, J. Adv. Mod. Earth Syst., 11, 257–277, https://doi.org/10.1029/2018ms001512, 2019.

Schumacher, R. S.: Sensitivity of precipitation accumulation in elevated convective systems to small changes in low-level moisture, J. Atmos. Sci., 72, 2507–2524, https://doi.org/10.1175/JAS-D-14-0389.1, 2015.

Schumacher, R. S. and Peters, J. M.: Near-surface thermodynamic sensitivities in simulated extreme-rain-producing mesoscale convective systems, Mon. Weather Rev., 145, 2177–2200, https://doi.org/10.1175/MWR-D-16-0255.1, 2017.

Seifert, A.: On the parameterization of evaporation of raindrops as simulated by a one-dimensional rainshaft model, J. Atmos. Sci., 65, 3608–3619, https://doi.org/10.1175/2008JAS2586.1, 2008.

https://doi.org/10.5194/egusphere-2026-1725
Preprint. Discussion started: 27 April 2026

Seifert, A., Khain, A., Blahak, U., and Beheng, K. D.: Possible effects of collisional breakup on mixed-phase deep convection simulated by a spectral (bin) cloud model, J. Atmos. Sci., 62, 1917–1931, https://doi.org/10.1175/jas3432.1, 2005.

Shpund, J., Khain, A., Lynn, B., Fan, J., Han, B., Ryzhkov, A., Snyder, J., Dudhia, J., and Gill, D.: Simulating a mesoscale convective system using WRF with a new spectral bin microphysics: 1: Hail vs graupel, J. Geophys. Res.-Atmos, 124, 14 072–14 101, https://doi.org/10.1029/2019JD030576, 2019.

Skamarock, W. C., Klemp, J. B., Dudhia, J., Gill, D. O., Liu, Z., Berner, J., Wang, W., Powers, J. G., Duda, M. G., Barker, D. M., and Huang, X.-Y.: A Description of the Advanced Research WRF Model Version 4, NCAR Tech. Note NCAR/TN-556+STR, p. 145, https://doi.org/10.5065/1dfh-6p97, 2019.

Sokolowsky, G. A., Freeman, S. W., Jones, W. K., Kukulies, J., Senf, F., Marinescu, P. J., Heikenfeld, M., Brunner, K. N., Bruning, E. C., Collis, S. M., Jackson, R. C., Leung, G. R., Pfeifer, N., Raut, B. A., Saleeby, S. M., Stier, P., and van den Heever, S. C.: *tobac* v1.5: Introducing fast 3D tracking, splits and mergers, and other enhancements for identifying and analysing meteorological phenomena, Geosci. Model Dev., 17, 5309–5330, https://doi.org/10.5194/gmd-17-5309-2024, 2024.

Sueki, K.: Massive parameter sweep experiment on convective cloud environment: changes in rainfall characteristics in moisture–instability–shear space, Sci. Online Lett. Atmos., 20B, 1–9, https://doi.org/10.2151/sola.20B-001, 2024.

Takemi, T.: A sensitivity of squall-line intensity to environmental static stability under various shear and moisture conditions, Atmos. Res., 84, 374–389, https://doi.org/10.1016/j.atmosres.2006.10.001, 2007.

Takemi, T.: Relationship between cumulus activity and environmental moisture during the CINDY2011/DYNAMO field experiment as revealed from convection-resolving simulations, J. Meteorol. Soc. Japan, 93A, 41–58, https://doi.org/10.2151/jmsj.2015-035, 2015.

Testud, J., Oury, S., Black, R. A., Amayenc, P., and Dou, X.: The concept of "Normalized" distribution to describe raindrop spectra: A tool for cloud physics and cloud remote sensing, J. Appl. Meteorol., 40, 1118–1140, https://doi.org/10.1175/1520-0450(2001)040<1118:TCONDT>2.0.CO;2, 2001.

Unuma, T.: Three-dimensional structure of an equilibrium drop size distribution within a convective system in Japan, Sci. Online Lett. Atmos., 20, 47–54, https://doi.org/10.2151/sola.2024-007, 2024.

Unuma, T.: Observed relationship between drop size distribution including a breakup signature and environmental properties near Kumagaya in eastern Japan, 25, 11 109–11 128, https://doi.org/10.5194/acp-25-11109-2025, 2025.

Unuma, T. and Takemi, T.: Characteristics and environmental conditions of quasi-stationary convective clusters during the warm season in Japan, Quart. J. Roy. Meteorol. Soc., 142, 1232–1249, https://doi.org/10.1002/qj.2726, 2016a.

Unuma, T. and Takemi, T.: A role of environmental shear on the organization mode of quasi-stationary convective clusters during the warm season in Japan, SOLA, 12, 111–115, https://doi.org/10.2151/sola.2016-025, 2016b.

Unuma, T., Yamauchi, H., Umehara, A., and Kato, T.: An equilibrium raindrop size distribution associated with a heavy-rain-producing convective system in Japan, Sci. Online Lett. Atmos., 19, 150–156, https://doi.org/10.2151/sola.2023-020, 2023.

Unuma, T., Yamauchi, H., Kato, T., Umehara, A., Hashimoto, A., Adachi, A., and Nagumo, N.: Characteristics of raindrop size distribution using 10-year disdrometer data in eastern Japan, J. Meteorol. Soc. Japan, 103, 219–232, https://doi.org/10.2151/jmsj.2025-011, 2025.

van der Walt, S., Schönberger, J. L., Nunez-Iglesias, J., Boulogne, F., Warner, J. D., Yager, N., Gouillart, E., Yu, T., and the scikit-image contributors: scikit-image: image processing in Python, PeerJ, 2, e453, https://doi.org/10.7717/peerj.453, 2014.

Wang, H., Xue, M., Yin, J., and Deng, H.: Comparison of simulated warm-rain microphysical processes in a record-breaking rainfall event using polarimetric radar observations, J. Geophys. Res.-Atmos, 128, e2023JD038 742, https://doi.org/10.1029/2023JD038742, 2023.

https://doi.org/10.5194/egusphere-2026-1725
Preprint. Discussion started: 27 April 2026

Xie, X., Evaristo, R., Troemel, S., Saavedra, P., Simmer, C., and Ryzhkov, A.: Radar observation of evaporation and implications for quantitative precipitation and cooling rate estimation, J. Atmos. Ocean. Technol., 33, 1779–1792, https://doi.org/10.1175/JTECH-D-15-0244.1, 2016.

Xue, L., Fan, J., Lebo, Z. J., Wu, W., Morrison, H., Grabowski, W. W., Chu, X., Geresdi, I., North, K., Stenz, R., Gao, Y., Lou, X., Bansemer, A., Heymsfield, A. J., McFarquhar, G. M., and Rasmussen, R. M.: Idealized simulations of a squall line from the MC3E field campaign applying three bin microphysics schemes: Dynamic and thermodynamic structure, Mon. Weather Rev., 145, 4789–4812, https://doi.org/10.1175/mwr-d-16-0385.1, 2017.